JOURNAL OF AGRICULTURAL AND FOOD CHEMISTRY

Biotransformation of Vinclozolin in Rat Precision-Cut Liver Slices: Comparison with *in Vivo* Metabolic Pattern

JULIAN BURSZTYKA, LAURENT DEBRAUWER, ELISABETH PERDU, ISABELLE JOUANIN, JEAN-PHILIPPE JAEG, AND JEAN-PIERRE CRAVEDI*

UMR1089 Xénobiotiques, INRA, F-31931 Toulouse, France

Vinclozolin is a dicarboxymide fungicide that presents antiandrogenic properties through its two hydrolysis products M1 and M2, which bind to the androgen receptor. Because of the lack of data on the biotransformation of vinclozolin, its metabolism was investigated *in vitro* in precision-cut rat liver slices and *in vivo* in male rat using [^{14}C]-vinclozolin. Incubations were performed using different concentrations of substrate, and the kinetics of formation of the major metabolites were studied. Three male Wistar rats were fed by gavage with [^{14}C]-VZ. Urine was collected for 24 h and analyzed by radio-HPLC for metabolic profiling. Metabolite identification was carried out on a LCQ ion trap mass spectrometer. In rat liver slices and *in vivo*, the major primary metabolite has been identified as 3′,5′-dichloro-2,3,4-trihydroxy-2-methylbutyranilide (M5) and was mainly present as glucurono-conjugates. M5 is produced by dihydroxylation of the vinyl group of M2. Other metabolites have been identified as 3-(3,5-dichlorophenyl)-5-methyl-5-(1,2-dihydroxyethyl)-1,3-oxazolidine-2,4-dione (M4), a dihydroxylated metabolite of vinclozolin, which undergoes further conjugation to glucuronic acid, and 2-[[(3,5-dichlorophenyl)-carbamoyl]oxy]-2-methyl-3,4-dihydroxy-butanoic acid (M6), a dihydroxylated metabolite of M1.

KEYWORDS: Vinclozolin; *in vitro* and *in vivo* metabolism; toxicology; endocrine disruptor

INTRODUCTION

Vinclozolin[3-(3,5-dichlorophenyl)-5-methyl-5-vinyl-1,3-oxazolidine-2,4-dione] is a nonsystemic dicarboxymide fungicide efficient in controlling plants or fruit diseases caused by *Botrytis* spp., *Monilia* spp., or *Sclerotinia* spp. Vinclozolin (VZ) undergoes spontaneous hydrolysis in aqueous media, giving three products, 2-[[(3,5-dichlorophenyl)-carbamoyl]oxy]-2-methyl-3-butenoic acid (M1), 3′,5′-dichloro-2-hydroxy-2-methylbut-3-enanilide (M2), and 3,5-dichloroaniline (M3) (*1*). M1 and M2 are responsible for the antiandrogenic effects attributable to vinclozolin since they competitively inhibit the binding of androgens to human androgen receptor (hAR) and inhibit androgen-induced gene expression *in vitro* and *in vivo* (*2, 3*). When administered during sexual differentiation, this fungicide has been shown to demasculinize and feminize the male rat offspring who display female-like anogenital distance at birth, retain nipples, a blind vaginal pouch, hypospadias, suprainguinal ectopic testes, and small to absent sex accessory glands (*4–6*). It has been demonstrated that VZ inhibits testosterone induced growth of androgen-dependent tissues (ventral prostate, seminal vesicles, and levator ani plus bulbocavernosus muscles) in a dose-additive manner in the Hershberger assay using castrated immature testosterone-treated rats (*7*). Hotchkiss et al. (*8*) also observed that neonatal injection of vinclozolin (200 mg/kg/day) demasculinized aggressive play behavior in male rats at 35 days of age, indicating that it altered CNS sexual differentiation in an antiandrogenic manner. Moreover, VZ can exert antiandrogenic effects in fish and mollusks, where this pesticide has been shown to cause a significant reduction of ejaculated sperm cells, smaller testes, and disrupted male courtship behavior in guppies (*Poecilia reticulate*) (*9*), and reduced penis length and accessory male sex organs in two prosobranch snails species, *Marisa cornuarietis* and *Nucella lapillus* (*10*). It has recently been demonstrated that embryonic exposure to VZ at the time of gonadal sex determination caused a transgenerational effect on male rat fertility and testis function (*11*). Adult animals from F1 to F4 generations developed a number of disease states or tissue abnormalities including prostate disease, kidney disease, immune system abnormalities, spermatogenesis abnormalities, breast tumor development, and blood abnormalities including hypercholesterolemia (*12*). The incidence or prevalence of these transgenerational disease states was high, from 10% for tumors to more than 50% for prostatic lesions in all generations, indicating that transgenerational effects were transmitted through epigenetic alterations (involving apparent permanent DNA methylation) in the male germline (i.e., sperm) (*13*).

Knowing the metabolic fate of VZ and its primary degradation products M1 and M2 in rat is of considerable interest to better understand the processes involved in the toxicological effects

* To whom correspondence should be addressed. Phone: +33 561 285 002. Fax: +33 561 285 244. E-mail: jcravedi@toulouse.inra.fr.

10.1021/jf0728045 CCC: $40.75
Published on Web 06/04/2008

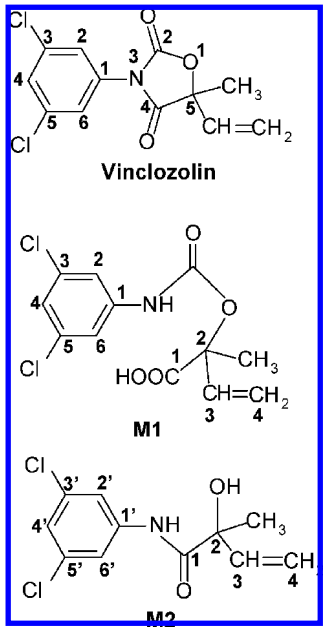

Figure 1. Structures of vinclozolin, M1, and M2.

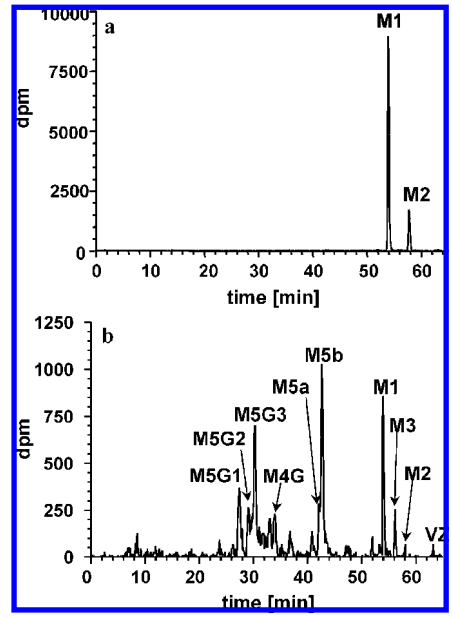

Figure 2. Typical radio-HPLC profile of [^{14}C]-vinclozolin metabolites present in rat liver slice culture medium (DMEM). Incubation and HPLC conditions were as described in the Materials and Methods section. Substrate final concentration was 10 μM. (**a**) Incubation without liver slices (6 h); (**b**) incubation with liver slices (6 h).

of this molecule. Since the sequential metabolic steps in precision-cut liver slices are similar to those occurring *in vivo* (*14*) and because the retention of heterogeneous cell population and liver architecture is close to the physiological situation *in vivo* (*15*), we used this *in vitro* model to study the metabolism of VZ in Wistar rats. Our investigations also include kinetic data. The *in vivo* metabolic profile of VZ was also examined in the urine of rats for comparison with the biotransformation pattern obtained *in vitro.*

MATERIALS AND METHODS

Chemicals. [Ring-U-^{14}C]-VZ was purchased from IZOTOP (Budapest, Hungary). Its specific activity was 71.17 MBq/mmol and its radiopurity ≥99%, as controlled by radio-HPLC. Unlabeled VZ was extracted from Ronilan (BASF France, Levallois-Perret) as described by Molina-Molina (*16*). Briefly, VZ was extracted with dichloromethane, and then the extract was evaporated to dryness, dissolved in methanol, and recrystallized. Solid vinclozolin was then ground to powder, and its purity was checked by melting point measurement on a Büchi 510 apparatus (108 °C corresponding to the value given in the literature) and was analyzed by HPLC coupled to a diode array detector (Spectra, Thermo Electron, Courtaboeuf, France). Its chemical purity was found to be greater than 97%. [^{14}C]-7-Ethoxycoumarin (7-EC) was purchased from Amersham (Buckinghamshire, UK). 7-EC, standard 3,5-dichloroaniline PESTANAL, Krebs-Henseleit buffer, and Dubelcco's modified eagle medium (DMEM) were from Sigma-Aldrich Chimie (Saint Quentin Fallavier, France).

Standard dihydroxylated M1, M2, and VZ on the vinyl group were chemically produced by catalytic amounts of osmium tetroxide with *N*-methylmorpholine *N*-oxide. The purified glycols were then analyzed by mass spectrometry, and their retention times were controlled by UV detection at 260 nm for comparison with metabolites.

All chemicals, solvents, and reagents for the preparation of buffers and HPLC eluents were of the highest grade commercially available from Merck (Nogent-sur-Marne, France). Ultrapure water from Milli-Q system (Millipore, Saint Quentin en Yvelines, France) was used for *in vitro* preparations and HPLC mobile phases.

Animals. Male Wistar rats weighing about 250 g were purchased from Iffa Credo (L'arbresle, France). Upon arrival at the animal facility, animals were allowed at least 1 week of acclimation prior to experimentation. Animals were given free access to laboratory diet (UAR 210; Villemoisson sur Orge, France) and tap water.

Liver Slice Preparation and Incubation. In each experiment, the animals were killed by cervical dislocation, followed by immediate exsanguination. Rat livers were perfused with 40 mL of ice-cold (4 °C) oxygenated Krebs-Henseleit buffer to remove blood. Liver cores were obtained using a stainless steel tube and drill press and immediately placed in ice-cold buffer. A Krumdieck tissue slicer (Alabama Research and Development Corp., Munford, AL) was used to produce precision-cut slices of 8 mm diameter and 0.2 mm thickness (*17*). An equilibration period of 45 min allowed for the sloughing of damaged cells and for recovery of Ca^{2+} and K^{+} homeostasis in the slices. At the end of incubations, the mean wet weight of slices was 20 mg, containing about 2 mg of protein. Slices were incubated in 12-well plastic tissue culture plates (*18*) using DMEM medium. The incubation volume was 1 mL. Plates were maintained at 37 °C in a rotary shaker, set at 90 rpm and saturated with a 95% O_2/5% CO_2 atmosphere. For each experiment, incubations were performed in triplicate using liver slices from three different rats. VZ was introduced dissolved into 2 μL of DMSO. In a first experiment, 6 incubation times (1, 2, 3, 4, 5, and 6 h) with one concentration (10 μM) of labeled VZ (3150 Bq/incubation) were tested. In a second experiment, 5 concentrations (5, 10, 50, 100, and 250 μM) of labeled VZ (3150 Bq/incubation) were incubated for 4 h. Blank samples were carried out by incubating 10 μM radiolabeled VZ (3150 Bq/incubation) in DMEM without rat liver slices in the conditions described above for 1 to 6 h. In each case, at the end of incubation, media samples were immediately harvested and stored at −20 °C until analysis.

Liver Slice Viability. 7-Ethoxycoumarin (7-EC) was used as a probe substrate for oxidative and conjugative metabolism, to assess the drug-metabolizing capacity of the rat liver slices. Control incubations were performed in triplicate using ^{14}C-labeled 7-EC 25 μM during 4 h for the rat liver slices.

***In Vivo* Metabolic Studies.** Three male rats were individually housed in metabolic cages. Animals were individually fed by gavage with 1 mg/kg [^{14}C]-VZ dissolved in DMSO and adjusted with unlabeled VZ to obtain a final activity of 0.481 MBq [^{14}C]-VZ/kg b.w. The final concentration of VZ in DMSO was 1 mg/mL. Urine was collected for 24 h and stored at −20 °C until analysis.

Analytical Procedure. All samples were individually thawed immediately before analysis. The radioactivity of each incubation medium was measured from aliquots (50 μL) by liquid scintillation counting in a Packard Tricarb 4430 counter with Ultima Gold (Packard Instruments Co., Downers Grove, IL) as the scintillation cocktail.

Aliquots (100 μL) of media samples from liver slice incubation or from rat urine were centrifuged for 5 min at 8600*g*, and the supernatant

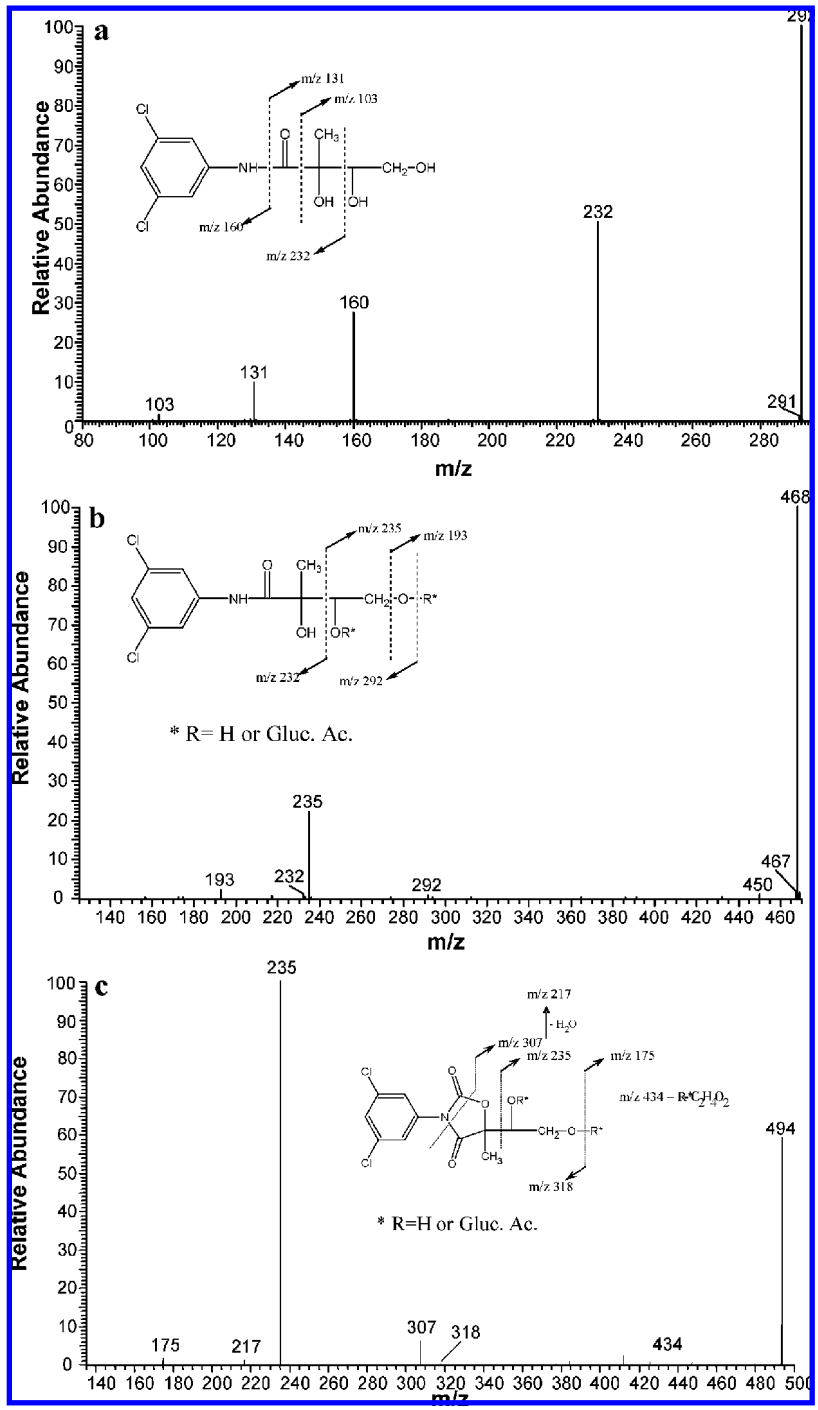

Figure 3. ESI-MS/MS mass spectra of M5 (**a**), M5 glucuronides (**b**), and M4 glucuronide (**c**).

was diluted with 400 μL of the corresponding HPLC system mobile phase A. HPLC coupled to online radioactivity detection (Flo-One A-500 instrument with Flo-scint II as scintillation cocktail, Packard Instrument Co.) was used for metabolite profiling. HPLC separations were performed on a Kromasil C18 column (250 × 4.6 mm, 5 μm) coupled to a Nucleodur C8 column (250 × 4.6 mm, 5 μm). The C18 column was protected by a Kromasil C18 guard precolumn (18 × 4.6 mm, 5 μm). Collection of radioactive peaks for MS analysis was carried out with a Gilson Model 202 fraction collector (Gilson, Villiers-Le-Bel, France). Briefly, 5 fractions per minute were obtained. For each of the main peaks, only the fraction in the middle of the peak was purified for further analysis.

The mobile phases consisted of ammonium acetate buffer (20 mM, pH 3.5) and acetonitrile 80:20 v/v in A and 30:70 v/v in B. The flow rate was 0.7 mL, and the temperature was 35 °C. The gradient used was 0−41 min linear gradient from 0% to 40% B, 41 to 44 min linear gradient from 40% to 90% B, 44 to 49 min linear gradient from 90% to 100% B, 49 to 66 min linear gradient from 100% B, and 66 to 81 min linear gradient from 100% B to 100% A. Metabolites were quantified by integrating the area under the radioactivity detected peaks.

Biotransformation of [3-^{14}C]-7-EC to radiolabeled 7-hydroxycoumarin, 7-hydroxycoumarin sulfate, and 7-hydroxycoumarin glucuronide was analyzed by radio-HPLC as previously described (*19*).

Metabolite Identification. Analyses were carried out on a quadrupole ion trap mass spectrometer (Finnigan LCQ, Thermo Finnigan, Les Ulis, France) fitted with an electrospray ionization source operating in the negative ion mode. Samples (typically 0.3−1 ng/μL in methanol−water (50−50, v/v)) were directly introduced into the ionization source via a syringe pump operating at a flow rate of 5 μL/min. The heated capillary was maintained at 200 °C. Typical operating parameters for production and transmission of electrospray produced ions into the ion trap analyzer were needle voltage 4.8−5.3 kV, nebulizing gas flow rate 40 arb-units,

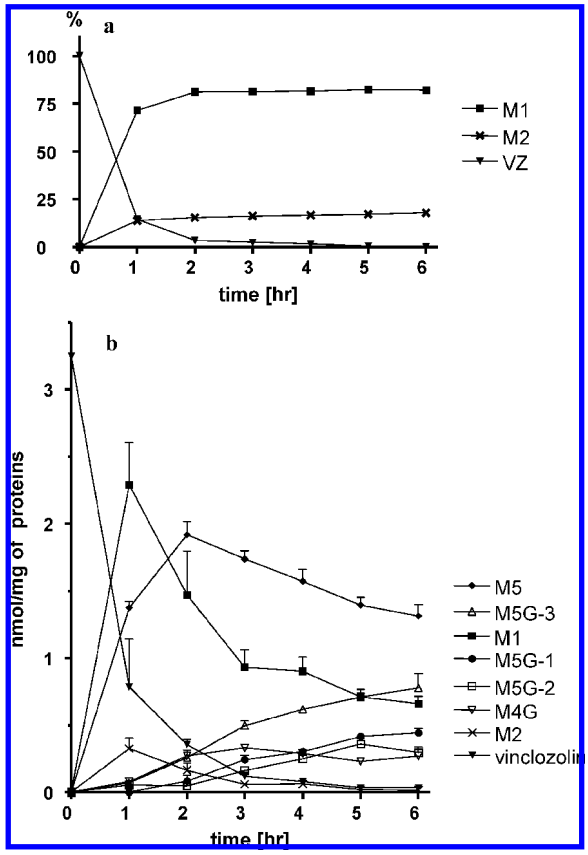

Figure 4. Time course study of the hydrolysis/biotransformation of vinclozolin. (**a**) Spontaneous hydrolysis of vinclozolin in DMEM at 37 °C. (**b**) Metabolism of vinclozolin in precision-cut rat liver slices. The concentration of vinclozolin in the incubation medium (DMEM) was 10 μM. The values are the means of three rats, and the error bars correspond to SD.

transfer capillary voltage −30 to +10 V, and tube lens offset −35 to +10 V. Other parameters for MS/MS experiments were as follows: isolation width 1 amu and excitation time 30 ms. Excitation voltage was adjusted for each compound in order to get maximum structural information for the compound of interest (typically 0.8−1.2 V_{p-p}). All analyses were achieved under automatic gain control conditions using helium as damping as well as collision gas for MS/MS experiments.

Data Analysis. Data analysis was conducted using an unpaired Student's *t*-test using Instat (Graph Pad software). Differences were considered significant if $P < 0.05$. K_m and V_{max} values were determined by nonlinear regression analysis as indicated by Loft and Poulsen (*20*).

RESULTS

Metabolism of Vinclozolin in Rat Liver Slices. After incubation of radiolabeled VZ with the precision-cut liver slices, about 80% of the initial radioactivity was found in the incubation media for all the concentrations tested. No further analysis was undertaken on the radiolabeled material remaining in the slices.

The qualitative and quantitative results obtained with incubation of 7-EC with rat liver slices were in accordance with those reported previously (*21*) with more than 50% of 7-EC metabolized in 4 h into 7-hydroxycoumarine, 7-hydroxycoumarine-glucuronide, and 7-hydroxycoumarine-sulfate, indicating a good metabolic capacity of the rat liver slices used.

Identification of Metabolites. The radio-HPLC analysis of the media control incubation revealed that about 85% of VZ was hydrolyzed after only 1 h in DMEM at 37 °C, giving two breakdown products; after 6 h, the parent compound was totally hydrolyzed (**Figure 2**). These products were identified by ESI-MS/MS and by comparison with data from the literature (*1, 22*). The major one (R_T = 53.8 min) gave an $[M - H]^-$ ion at *m/z* 302 and characteristic fragment ions at *m/z* 258, 175, and 115, corresponding to M1. The NI-ESI-MS spectrum of the second one (R_T = 58 min) displayed an $[M - H]^-$ ion at *m/z* 258 whose MS/MS analysis gave a fragment ion at *m/z* 160 diagnostic of M2. No other degradation products were observed.

Biotransformation of VZ by rat liver slices was extensive (**Figure 2**). The radio-HPLC profiles obtained in our experimental conditions were qualitatively similar whatever the concentration tested or the duration of incubation. Collection of the radioactive peaks was carried out prior to MS analysis of metabolites. The identification of metabolites was performed only on 100 μM incubations.

Peaks M5a and M5b (R_T = 42.6 and 43 min) were incompletely separated and gave the same $[M - H]^-$ ion at *m/z* 292 accompanied by the isotopic contribution of the ^{37}Cl atoms giving an ion at *m/z* 294. After isolation and fragmentation of the *m/z* 292 precursor ion into the ion trap device, the MS/MS spectrum presented in **Figure 3a** was obtained. Diagnostic fragment ions were observed at *m/z* 103, 131, 160, and 232. The complementary fragment ions at *m/z* 160 and 131 correspond to the cleavage of the amide bond of M5 with negative charge retention being possible on both sides of the molecule. α-Cleavages of the tertiary alcohol explain the occurrence of the fragment ions at *m/z* 103 and 232, respectively. On the basis of these data, peaks M5a and M5b could be identified as two different forms (likely diastereoisomers) of 3′,5′-dichloro-2,3,4-trihydroxy-2-methylbutyranilide (M5). In order to confirm this identification, a chemical hydroxylation of M2 was carried out using osmium tetroxyde. The resulting compound displayed a R_T of 42.6 min. when injected in the same HPLC system. The corresponding MS and MS/MS spectra were super imposable with those obtained for M5a.

The negative ESI mass spectrum of peaks M5G1, M5G2 and M5G3 (R_T = 27.6, 29.2 and 30.3 min respectively) gave an intense signal at *m/z* 468 with the characteristic isotopic pattern of a doubly chlorinated molecule (i.e., *m/z* 470 present at ca. 65% intensity relative to *m/z* 468). The MS/MS spectrum of the *m/z* 468 precursor ion of the first peak is presented in **Figure 3b**. It displays characteristic fragment ions at *m/z* 193, 232, 235, and 292, which could be attributed to the fragmentation pattern presented in **Figure 3b**. These characteristic fragment ions allowed us to identify M5G1 as a glucuronic acid conjugate of M5. The *m/z* 235 fragment ion allowed us to rule out the glucuronidation on the tertiary alcohol group of M5. However, on the basis of the structural information available on the MS/MS spectrum, we were not able to determine the position of glucuronidation, which may concern either the primary or the secondary hydroxyl function of M5. The MS/MS spectra obtained from the *m/z* 468 ion of M5G2 and M5G3 were identical to that of M5G1. Thus, these peaks also corresponded to M5 glucuronides. The presence of several peaks for M5 glucuronides can be attributed to (i) the two possible positions of glucuronidation evidenced by MS/MS analysis and (ii) the occurrence of diastereoisomeric forms of M5 glucuronide, which may be separated by reversed phase HPLC.

The isotopic pattern of a chlorinated metabolite was located at *m/z* 494/496 on the NI-ESI mass spectrum of peak M4G (R_T = 34 min). For getting structural information, the *m/z* 494 ion was selected and submitted to resonant excitation in an MS/MS experiment (**Figure 3c**). The main resulting fragment ions were produced at *m/z* 235 and 307. A weak signal was also observed at *m/z* 175, suggesting the occurrence of a glucuronic

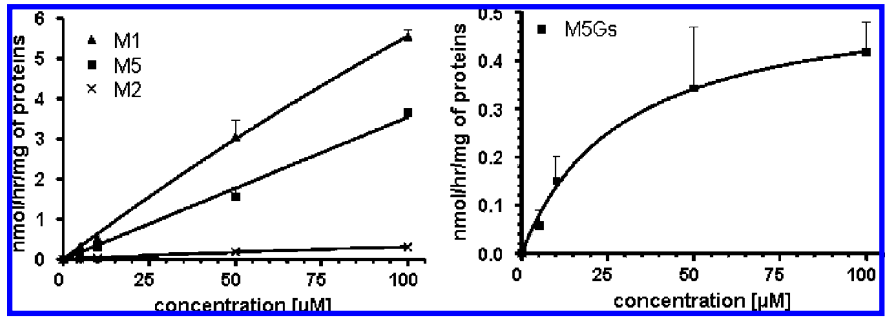

Figure 5. Michaelis−Menten plots of vinclozolin biotransformation in precision-cut rat liver slices. Slices were incubated for 4 h with various concentrations of vinclozolin. The values are the means of three rats, and the error bars correspond to SD. (**Left**) Formation of M1, M2, and M5. (**Right**) Formation of M5 glucuronides (total glucuronides of M5 were measured for calculations).

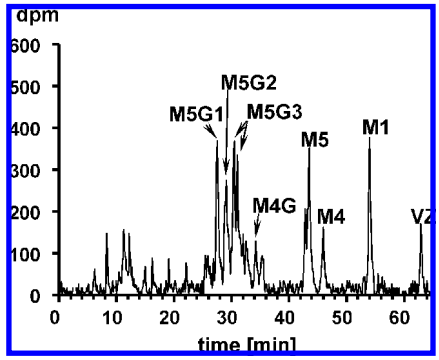

Figure 6. Zero to 24 h urinary radio-HPLC profile from rats force-fed a single dose of [^{14}C]-vinclozolin (1 mg/kg bw).

acid conjugate. The *m/z* 235 fragment ion could reasonably present the same structure as that indicated for M5 glucuronide (see **Figure 3**). The formation of the *m/z* 307 ion can result in the cleavage of the five-membered heterocycle considering that no metabolic ring opening occurred on VZ in this case. Thus, this peak was identified as the glucuronic acid conjugate of 3-(3,5-dichlorophenyl)-5-methyl-5-(1,2-dihydroxyethyl)-1,3-oxazolidine-2,4-dione (M4).

M3 coeluted with standard 3,5-dichloroaniline (R_T = 56.2 min) monitored by UV detection at 212 nm.

Kinetics of VZ Hydrolysis and Metabolism in Rat Liver Slices. The hydrolysis time course of VZ in DMEM at 37 °C is shown in **Figure 4a**. VZ is almost totally hydrolyzed in 2 h, giving M1 (about 80%) and M2 (about 20%).

The kinetics of formation of [^{14}C]-VZ metabolites by rat liver slices is shown in **Figure 4b**. The amount of VZ in incubation media rapidly decreased and represented about 15% of total radioactivity after 1 h, about 6% after 2 h, and less than 2% after 4 h. The amounts of M1 and M2 reached the maximum values after about 1 h, accounting for more than 34% of total radioactivity for M1 and 4% for M2, whereas for M5, the maximum values were reached after about 2 h, corresponding to about 36% of the total radioactivity. After reaching the maximum values, a steady decrease of the concentrations of these three metabolites was observed, M1 accounting for 12% of the total radioactivity at 6 h of incubation, M5 still representing more than 21% at the same sampling time, whereas only traces of M2 were detected. After 2 h, M5 was the major metabolite at all time points. M5-glucuronides (M5G1, M5G2, and M5G3) increased after about 1 h to represent 33% of the total radioactivity after 6 h. M4G increased to represent about 6% of the total radioactivity after 3 h of incubation. 3,5-Dichloroaniline represented between 2 and 3% of the total radioactivity present in incubation media at all time points (data not shown).

Metabolite formation over the concentration range is shown in **Figure 5**. Because of an incomplete solubilization of VZ at 250 μM, the results corresponding to this concentration were not represented. M1 and M5 formations were linear up to 100 μM in precision-cut liver slices (**Figure 5**, **left**). M2 appeared to be produced under saturation kinetics with apparent V_{max} = 1.22 ± 0.92 nmol/h/mg of protein. However, M1 and M2 are produced by nonenzymatic hydrolysis of VZ; thus, the saturation-look of M2 production is due to its biotransformation into M5 and M5 glucuronides, while its production is limited by the VZ hydrolysis into M1. M5 conjugation to glucuronide acid over the concentration range is represented in **Figure 5**, **right**. Since separation of the M5G1, M5G2, and M5G3 peaks did not allow a precise quantification of these metabolites, the kinetic data were calculated by using the sum of the glucuronide conjugates produced from M5 (M5Gs) at each concentration. Total M5Gs were produced under saturation kinetics with apparent V_{max} = 0.54 ± 0.14 nmol/h/mg of protein and K_m = 29.14 ± 20.76 μM.

Identification of Urinary Metabolites. An average of 24% of the administered radioactivity was found in 0−24 h urine samples. The radio-HPLC profile corresponding to pooled urine samples of male rat urine 24 h after being force fed is shown in **Figure 6**. The major metabolites were identified by ESI/MS-MS as M5G1, M5G2, M5G3, M4G, M5, and M1. Several additional peaks corresponding to polar compounds were detected at elution times between 8 and 14 min. Probably because of an incomplete separation of several minor metabolites, we failed to identify these compounds. Another additional peak was detected at R_T = 46 min. Its analysis by negative ESI-MS gave a signal corresponding to the $[M - H]^-$ ion of two dichlorinated species at *m/z* 318/320 and *m/z* 336/338. By MS/MS analysis, the *m/z* 318 ion yielded main characteristic fragment ions at *m/z* 160, 258, and 274. The first one corresponded to the deprotonated form of dichloroaniline, whereas the *m/z* 258 and 274 fragment ions resulted in the elimination of HO-CH=CH-OH and CO_2, respectively, from the *m/z* 318 $[M - H]^-$ precursor ion. These data supported the identification of this peak as 3-(3,5-dichlorophenyl)-5-methyl-5-(1,2-dihydroxyethyl)-1,3-oxazolidine-2,4-dione (M4). This was also confirmed by LC and MS/MS analysis of the glycol resulting from the chemical hydroxylation of VZ by osmium tetroxyde, which gave both a R_T of 46 min and the same fragment ions as M4 after MS/MS analysis of the *m/z* 318 precursor ion. Besides, the MS/MS spectrum of the *m/z* 336 ion displayed a unique fragment ion at *m/z* 149. The chemical hydroxlation of M1 by osmium tetroxyde gave a compound with a R_T of 46 min, also displaying an $[M - H]^-$ isotopic cluster at *m/z* 336/338. The MS/MS analysis of the *m/z* 336 ion also yielded a unique fragment ion at *m/z* 149, corresponding to the

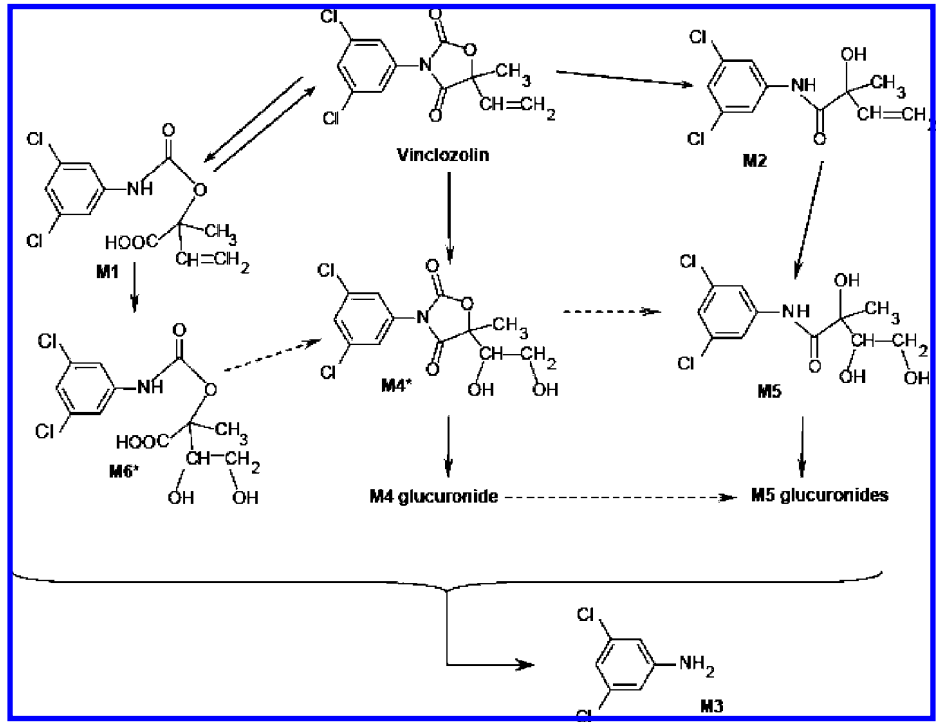

Figure 7. Proposed metabolic pathways of the *in vitro* (precision-cut rat liver slices) and *in vivo* biotransformation of vinclozolin. (*) Only present in rat urine.

cleavage of the ester function of this compound with charge retention on the nonaromatic part of the molecule. On the basis of the comparison of both retention time and MS/MS spectra, this metabolite was identified as 2-[[(3,5-dichlorophenyl)-carbamoyl]oxy]-2-methyl-3,4-dihydroxy-butanoic acid (M6). From 24 h after the force-feeding, M5 and its conjugates to glucuronic acid were the major metabolites present in urine with M1.

DISCUSSION

The present study characterizing VZ metabolites produced *in vitro* in liver slices and *in vivo* provides evidence that VZ and corresponding breakdown products are efficiently biotransformed by rats.

Spontaneous hydrolysis of VZ occurred in the incubation medium without slices. This result was expected since the hydrolysis of VZ in various aqueous buffers was described by Szeto et al. (*1*). These authors demonstrated that the reaction was base-catalyzed and that the rate of hydrolysis was proportional to pH. At 35 °C and pH 7.0, 10% of VZ (40 μM) hydrolyzed after 1 h to yield M1 (8.5%) and M2 (1.5%), whereas at pH 8.0, 47% of VZ was converted to M1 (39%) and M2 (8%) after 1 h. In our experimental conditions (incubations in DMEM without slices) and after the same period of time, M1 and M2 accounted for 72 and 13% of total radioactivity, respectively, suggesting that the conversion of VZ to M1 and M2 could also be partly due to DMEM catalysis of the reaction. M3 could not be observed because the incubation times were too short (*1*).

Although the chemical conversion of VZ to M1 is known to be reversible, the formation of VZ from M1 by recyclization only occurs at a significant extent at acidic pH (*1*). Taking into consideration that our incubations were undertaken at pH 7.4, it was likely that only very minute amounts of M1, if any, could be converted back to VZ. When incubations were performed with liver slices, the concentration of M1 increased steadily to a maximum after 1 h and decreased gradually thereafter. We observed that a dihydroxyladed metabolite of M1 (M6) can be produced. However, no phase II metabolites originating from M1 were identified, and the amount of M6 produced could not explain the decrease in M1 amount. This result could be explained by the recyclization of M6 to give M4, which can undergo hydrolysis to give M5 (data not shown). It is also possible that M6 undergoes further biotransformation into unidentified metabolites. Moreover, the rapid biotransformation of M2 could result in a concomitant hydrolysis of VZ to M2, favoring the subsequent conversion of M1 to VZ. At the same time, M2 is always present in very small amounts because it is readily metabolized, giving M5 and M5 glucuronides. After 6 h, VZ and M2 were present only in trace amounts, while glucuronides of M5 and M4 represented about 33% of the total radioactivity.

The major metabolic pathways of VZ are summarized in **Figure 7**. The same metabolites involving phase I and phase II enzymes are characterized from rat urine and from rat liver slices. The first step is the hydrolytic opening of the oxazolidine ring, involving nonenzymatic cleavage of the 2-, 3-, or 3,4-nitrogen−carbon bonds, to give M2 and M1 compounds, respectively. Cleavage of the 2,3-nitrogen−carbon bond is followed by decarboxylation and is not reversible, in contrast to the cleavage of the 3,4-nitrogen−carbon bond (*1*). The enzymatic phase-I step includes the dihydroxylation of the vinyl group, presumably via an epoxyde intermediate, resulting in metabolite M4 from VZ, metabolite M5 from M2, and M6 from M1. Phase-II pathways include extensive conjugation to glucuronic acid of the dihydroxylated M4 and M5 compounds, giving three glucuronoconjugates. These pathways are in agreement with those reported previously in unpublished reports (*23*). M5 has also been reported as a fungal metabolite of VZ (*24*). M5 can be obtained also from M4 by hydrolytic cleavage of the 2,3-nitrogen−carbon bond. Moreover, the same hydrolysis could happen with M4 conjugates, giving M5 conjugates,

explaining that the major metabolites identified in rat liver slice incubation media are M5 and M5 conjugates. On the basis of the R_T of standard 3,5-dichloroaniline, M3 seemed to be present only in precision-cut rat liver slice incubation media. M3 is a well described end product of VZ degradation (*1, 25*) but was not detected in rat urine, probably because 3,5-dichloroaniline undergoes further biotransformation, such as hydroxylation and conjugation to glucuronic acid (*26*).

In vitro and *in vivo*, the major metabolites identified are M1 (hydrolysis product), M5 (dihydroxylated metabolite from M2), and M5 glucurono-conjugates, and to a lesser extent M4 and its glucuronoconjugate. VZ antiandrogenic activity is described to be mainly due to M2 and M1 since they compete with [17 α-methyl]-methyltrienolone (R1881) for the androgen receptor with a K_i of 9.7 and 92 μM, respectively, that is about 100- and 10-fold more effective than VZ itself (*3*).

Data on the fate of VZ in humans are also scarce. The presence of VZ residues in human serum and urine was investigated recently (*27–31*). In some cases, only VZ was determined, whereas in others, the sum VZ + metabolites was estimated, on the basis of the quantification of 3,5-dichloroaniline, determined after basic or acidic hydrolysis of the samples. No data on the metabolic pathways of VZ in humans were identified.

This is the first published study on the metabolic fate of VZ in rats *in vivo* and *in vitro*, including identification of the major metabolites and kinetics of biotransformation. It demonstrates that M1 and M2, which are mainly responsible of the antiandrogenic effects attributable to VZ, are not the end products of the biotransformation of VZ in rats. VZ and M2 are quickly biotransformed by dihydroxylation of the vinyl group and by further conjugation to glucuronic acid. The activity of these metabolites toward the androgen receptor remains to be definitively established.

ABBREVIATIONS USED

AR, androgen receptor; CNS, central nervous system; DMEM, Dubelcco's modified eagle medium; DMSO, dimethyl sulfoxide; 7-EC, 7-ethoxycoumarin; ESI, electrospray ionization; HPLC, high-performance liquid chromatography; LC-MS, combined high-performance liquid chromatography/mass spectrometry; MS, mass spectrometry; *RT*, retention time; UV, ultraviolet; VZ, vinclozolin.

ACKNOWLEDGMENT

We thank Florence Blas y Estrada and Raymond Gazel for animal care.

LITERATURE CITED

(1) Szeto, S. Y.; Burlinson, N. E.; Rahe, J. E.; Oloffs, P. C. Kinetics of hydrolysis of the dicarboximide fungicide vinclozolin. *J. Agric. Food Chem.* **1989**, *37*, 523–529.

(2) Kelce, W.; Monosson, R.; Gamcsik, E.; Laws, M. P.; Gray, S. C.; L. E. Jr. Environmental hormone disruptors: evidence that vinclozolin developmental toxicity is mediated by antiandrogenic metabolites. *Toxicol. Appl. Pharmacol.* **1994**, *126*, 276–85.

(3) Kelce, W. R.; Lambright, C. R.; Gray, L. E., Jr.; Roberts, K. P. Vinclozolin and p,p′-DDE alter androgen-dependent gene expression: in vivo confirmation of an androgen receptor-mediated mechanism. *Toxicol. Appl. Pharmacol.* **1997**, *142*, 192–200.

(4) Gray, L. E., Jr.; Ostby, J. S.; Kelce, W. R. Developmental effects of an environmental antiandrogen: the fungicide vinclozolin alters sex differentiation of the male rat. *Toxicol. Appl. Pharmacol.* **1994**, *129*, 46–52.

(5) Shono, T.; Suita, S.; Kai, H.; Yamaguchi, Y. The effect of a prenatal androgen disruptor, vinclozolin, on gubernacular migration and testicular descent in rats. *J. Pediatr. Surg.* **2004**, *39*, 213–6.

(6) Shono, T.; Suita, S.; Kai, H.; Yamaguchi, Y. Short-time exposure to vinclozolin in utero induces testicular maldescent associate with a spinal nucleus alteration of the genitofemoral nerve in rats. *J. Pediatr. Surg.* **2004**, *39*, 217–9, discussion 217−9.

(7) Kang, I. H.; Kim, H. S.; Shin, J. H.; Kim, T. S.; Moon, H. J.; Kim, I. Y.; Choi, K. S.; Kil, K. S.; Park, Y. I.; Dong, M. S.; Han, S. Y. Comparison of anti-androgenic activity of flutamide, vinclozolin, procymidone, linuron, and p,p′-DDE in rodent 10-day Hershberger assay. *Toxicology* **2004**, *199*, 145–59.

(8) Hotchkiss, A. K.; Ostby, J. S.; Vandenbergh, J. G.; Gray, L. E., Jr. An environmental antiandrogen, vinclozolin, alters the organization of play behavior. *Physiol. Behav.* **2003**, *79*, 151–6.

(9) Baatrup, E.; Junge, M. Antiandrogenic pesticides disrupt sexual characteristics in the adult male guppy *Poecilia reticulata*. *Environ. Health. Perspect.* **2001**, *109*, 1063–70.

(10) Tillmann, M.; Schulte-Oehlmann, U.; Duft, M.; Markert, B.; Oehlmann, J. Effects of endocrine disruptors on prosobranch snails Mollusca: Gastropoda) in the laboratory. Part III: Cyproterone acetate and vinclozolin as antiandrogens. *Ecotoxicology* **2001**, *10*, 373–88.

(11) Anway, M. D.; Cupp, A. S.; Uzumcu, M.; Skinner, M. K. Epigenetic transgenerational actions of endocrine disruptors and male fertility. *Science* **2005**, *308*, 1466–9.

(12) Anway, M. D.; Leathers, C.; Skinner, M. K. Endocrine disruptor vinclozolin induced epigenetic transgenerational adult-onset disease. *Endocrinology* **2006**, *147*, 5515–23.

(13) Chang, H. S.; Anway, M. D.; Rekow, S. S.; Skinner, M. K. Transgenerational epigenetic imprinting of the male germline by endocrine disruptor exposure during gonadal sex determination. *Endocrinology* **2006**, *147*, 5524–41.

(14) Parrish, A. R.; Gandolfi, A. J.; Brendel, K. Precision-cut tissue slices: applications in pharmacology and toxicology. *Life Sci.* **1995**, *57*, 1887–901.

(15) Ekins, S.; Williams, J. A.; Murray, G. I.; Burke, M. D.; Marchant, N. C.; Engeset, J.; Hawksworth, G. M. Xenobiotic metabolism in rat, dog, and human precision-cut liver slices, freshly isolated hepatocytes, and vitrified precision-cut liver slices. *Drug. Metab. Dispos.* **1996**, *24*, 990–5.

(16) Molina-Molina, J. M.; Hillenweck, A.; Jouanin, I.; Zalko, D.; Cravedi, J. P.; Fernandez, M. F.; Pillon, A.; Nicolas, J. C.; Olea, N.; Balaguer, P. Steroid receptor profiling of vinclozolin and its primary metabolites. *Toxicol. Appl. Pharmacol.* **2006**, *216*, 44–54.

(17) Krumdieck, C. L.; dos Santos, J. E.; Ho, K. J. A new instrument for the rapid preparation of tissue slices. *Anal. Biochem.* **1980**, *104*, 118–23.

(18) Dogterom, P. Development of a simple incubation system for metabolism studies with precision-cut liver slices. *Drug. Metab. Dispos.* **1993**, *21*, 699–704.

(19) Zalko, D.; Perdu-Durand, E.; Debrauwer, L.; Bec-Ferte, M. P.; Tulliez, J. Comparative metabolism of clenbuterol by rat and bovine liver microsomes and slices. *Drug. Metab. Dispos.* **1998**, *26*, 28–35.

(20) Loft, S.; Poulsen, H. E. Metabolism of metronidazole and antipyrine in isolated rat hepatocytes. Influence of sex and enzyme induction and inhibition. *Biochem. Pharmacol.* **1989**, *38*, 1125–36.

(21) Ekins, S.; Murray, G. I.; Burke, M. D.; Williams, J. A.; Marchant, N. C.; Hawksworth, G. M. Quantitative differences in phase I and II metabolism between rat precision-cut liver slices and isolated hepatocytes. *Drug. Metab. Dispos.* **1995**, *23*, 1274–9.

(22) Dhananjeyan, M. R.; Erhardt, P. W.; Corbitt, C. Simultaneous determination of vinclozolin and detection of its degradation products in mouse plasma, serum and urine, and from rabbit bile, by high-performance liquid chromatography. *J. Chromatogr., A* **2006**, *1115*, 8–18.

(23) Watson, W. Vinclozolin Pesticide Residues in Food: 1995 Evaluations. Part II: Toxicological & Environmental. IPCS INCHEM, 1995. http://www.inchem.org/documents/jmpr/jmpmono/v95pr18.htm.

(24) Pothuluri, J. V.; Freeman, J. P.; Heinze, T. M.; Beger, R. D.; Cerniglia, C. E. *J. Agric. Food Chem.* **2000**, *48*, 6138–6148.

(25) Cabras, P.; Diana, P.; Meloni, M.; Pirisi, F. M.; Pirisi, R. Reversed-phase high-performance liquid chromatography of pesticides. VII. Analysis of vinclozolin, iprodione, procymidone, dichlozolinate and their degradation product 3,5-dichloroaniline on white must and wine extracts. *J. Chromatogr.* **1983**, *256*, 176–81.

(26) Valentovic, M. A.; Lo, H. H.; Brown, P. I.; Rankin, G. O. 3,5-Dichloroaniline toxicity in Fischer 344 rats pretreated with inhibitors and inducers of cytochrome P450. *Toxicol. Lett.* **1995**, *78*, 207–14.

(27) Carlucci, G.; Pasquale, D. D.; Ruggieri, F.; Mazzeo, P. Determination and validation of a simple high-performance liquid chromatographic method for simultaneous assay of iprodione and vinclozolin in human urine. *J. Chromatogr., B* **2005**, *828*, 108–12.

(28) Lindh, C. H.; Littorin, M.; Amilon, A.; Jonsson, B. A. Analysis of 3,5-dichloroaniline as a biomarker of vinclozolin and iprodione in human urine using liquid chromatography/triple quadrupole mass spectrometry. *Rapid Commun. Mass Spectrom.* **2007**, *21*, 536–42.

(29) Moreno Frias, M.; Garrido Frenich, A.; Martinez Vidal, J. L.; Mateu Sanchez, M.; Olea, F.; Olea, N. Analyses of lindane, vinclozolin, aldrin, p,p′-DDE, o,p′-DDT and p,p′-DDT in human serum using gas chromatography with electron capture detection and tandem mass spectrometry. *J. Chromatogr., B* **2001**, *760*, 1–15.

(30) Turci, R.; Barisano, A.; Balducci, C.; Colosio, C.; Minoia, C. Determination of dichloroanilines in human urine by gas chromatography/mass spectrometry: validation protocol and establishment of Reference values in a population group living in central Italy. *Rapid Commun. Mass Spectrom.* **2006**, *20*, 2621–5.

(31) Wittke, K.; Hajimiragha, H.; Dunemann, L.; Begerow, J. Determination of dichloroanilines in human urine by GC-MS, GC-MS-MS, and GC-ECD as markers of low-level pesticide exposure. *J. Chromatogr., B* **2001**, *755*, 215–28.

Received for review September 20, 2007. Revised manuscript received April 14, 2008. Accepted April 15, 2008. This study has been partly supported by the European Union network CASCADE (FOOD-CT-2003-506319).

JF0728045